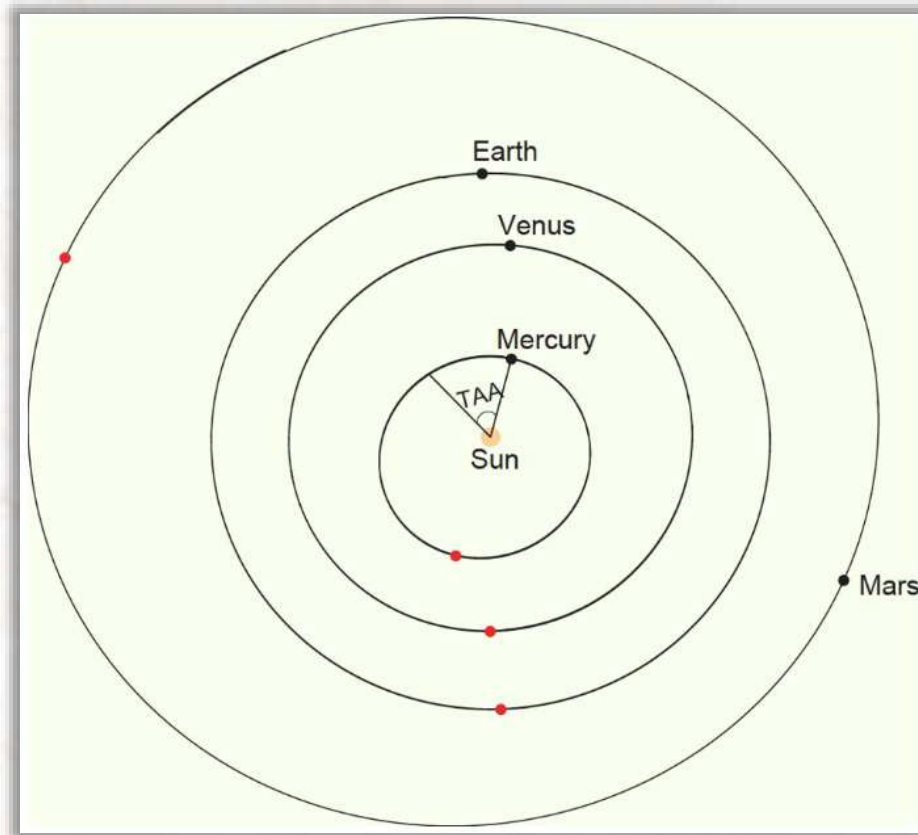
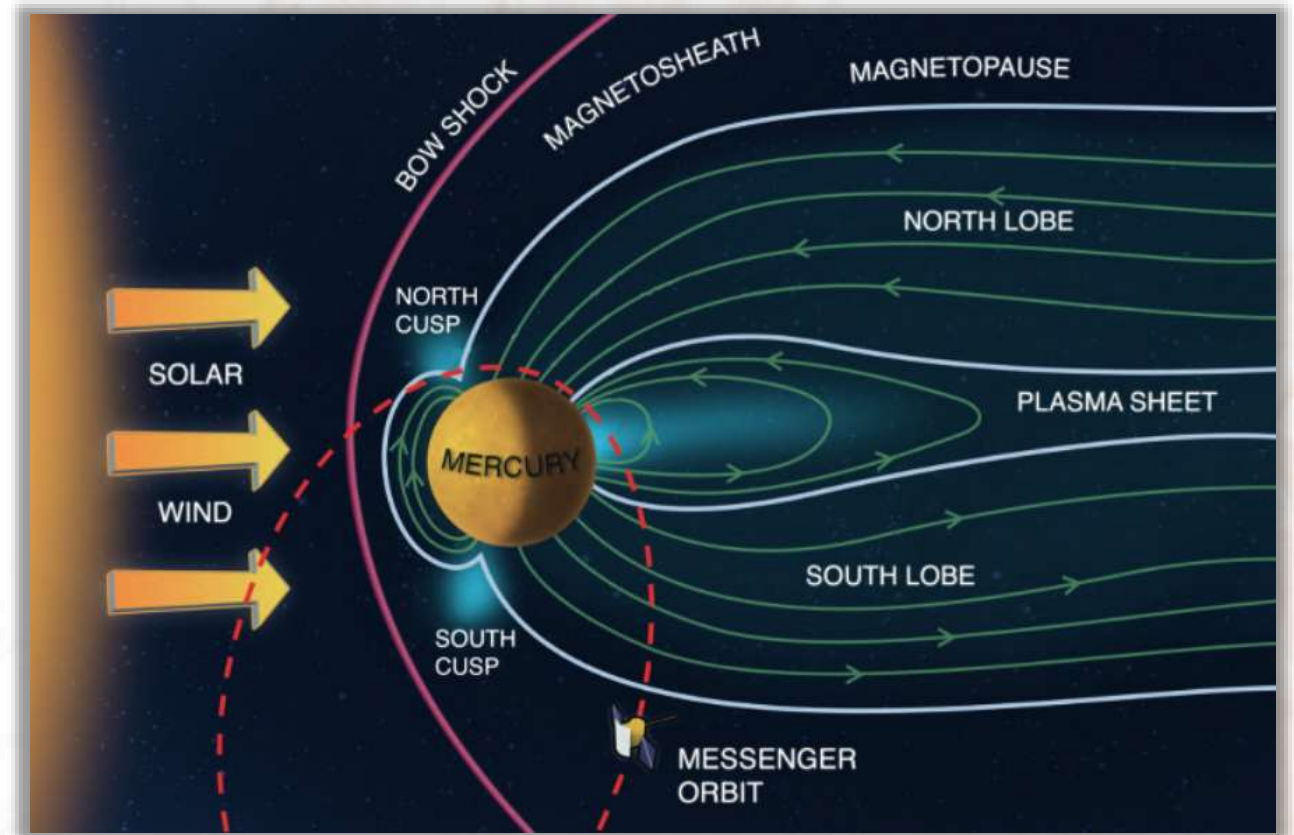


0 Dynamic Environment of Mercury's Magnetosphere

Position & Magnetosphere Structure

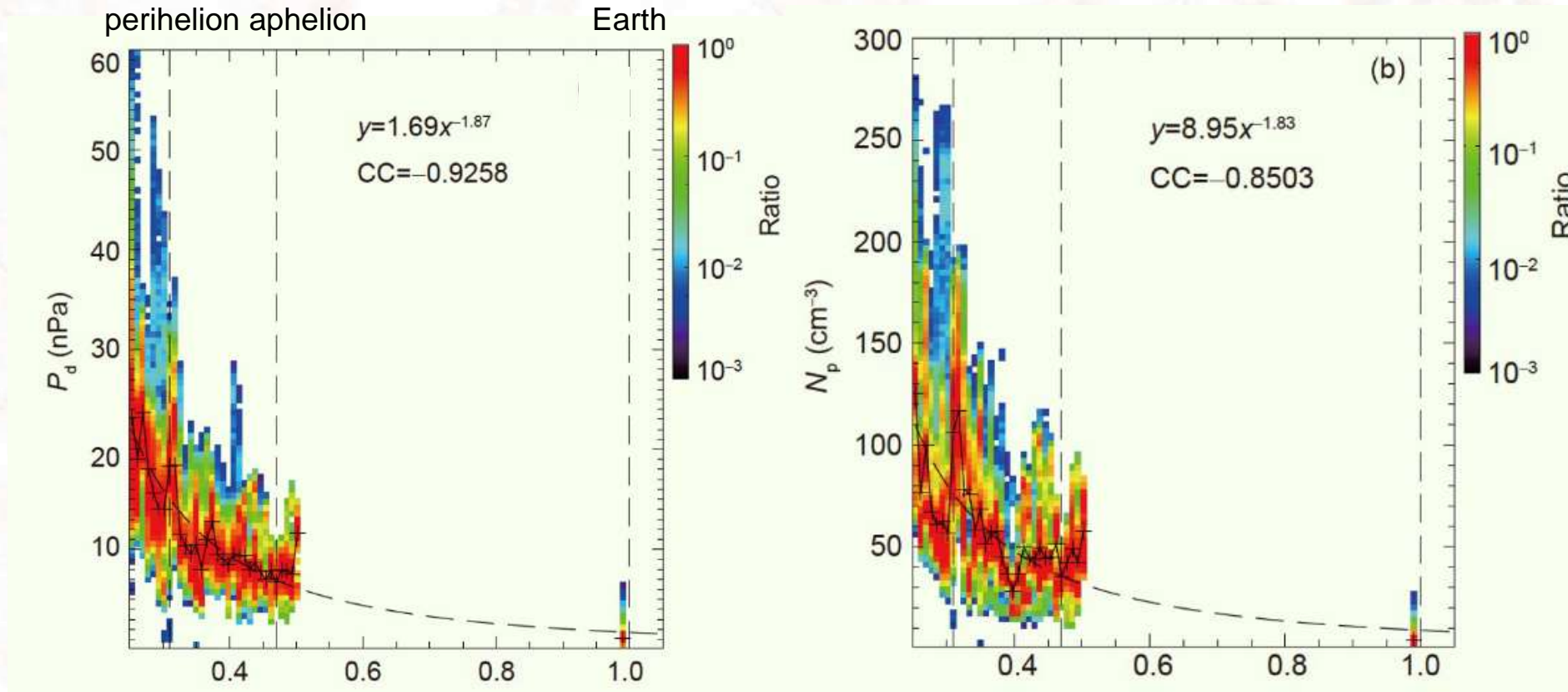


[Sun W et al., 2022]



[Zurbuchen et al., 2011]

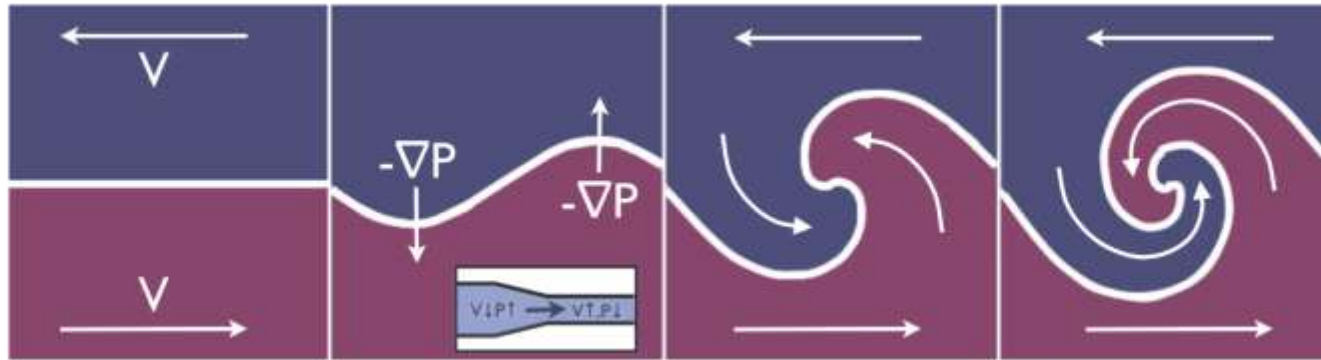
0 Dynamic Environment of Mercury's Magnetosphere



[Sun W et al., 2022]

- Solar wind dynamic pressure: ~3.5 to 9.0 nPa, **six to 10 times of Earth's** (~0.55 nPa)
- Solar wind density: ~30 to 120 cm⁻³, **six to 30 times of Earth's** (~4.5 cm⁻³)

1 Kelvin–Helmholtz Instability



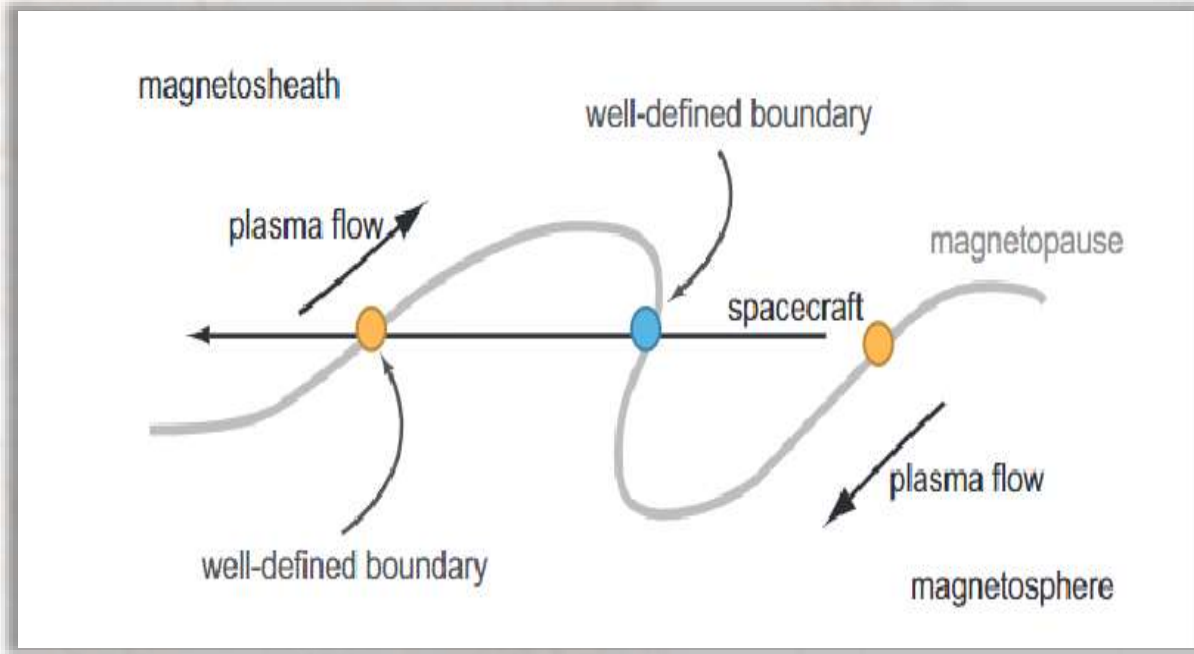
[J.R.Johnson et al., 2014]

- A velocity shear exists either within a single fluid or between two distinct fluids.
- Kelvin-Helmholtz (K-H) waves at the magnetopause are driven by velocity shear between magnetospheric and magnetosheath plasma flows

$$\omega = \frac{\mathbf{k} \cdot (\rho_{msh} \mathbf{V}_{msh} + \rho_{msp} \mathbf{V}_{msp})}{\rho_{msh} + \rho_{msp}} \pm i \sqrt{\left(\frac{\rho^*}{\rho_{msh} + \rho_{msp}} \right) \left([\mathbf{k} \cdot (\mathbf{V}_{msh} - \mathbf{V}_{msp})]^2 - \frac{(\mathbf{k} \cdot \mathbf{B}_{msh})^2 + (\mathbf{k} \cdot \mathbf{B}_{msp})^2}{4\pi\rho^*} \right)} \quad (1)$$

where ρ^* is a mean mass $\rho^* = \rho_{msh}\rho_{msp}/(\rho_{msh} + \rho_{msp})$ (msp/msh = magnetosphere/sheath).
K–H waves are unstable when $(\mathbf{k} \cdot (\mathbf{V}_{msh} - \mathbf{V}_{msp}))^2 > ((\mathbf{k} \cdot \mathbf{B}_{msh})^2 + (\mathbf{k} \cdot \mathbf{B}_{msp})^2)/4\pi\rho^*$.

2 How to pick up Kelvin–Helmholtz waves?



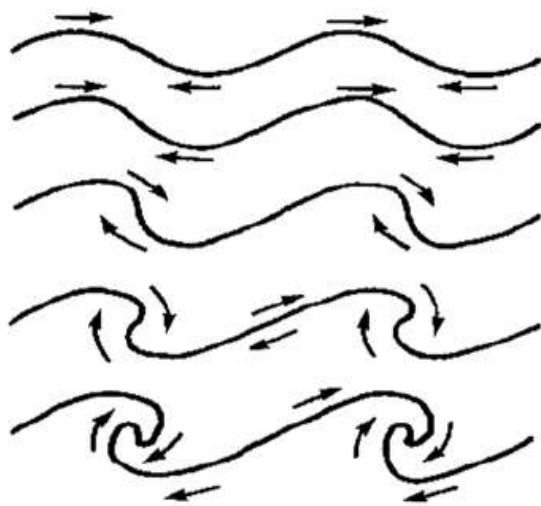
Due to the lack of direct flow measurements from MESSENGER, we identified Kelvin-Helmholtz (K-H) waves through variations in the **magnetic field, plasma density, and plasma temperature.**

[T. Sundberg et al., 2010]

Characteristics	Comparison
Magnetic field	Magnetosheath < Magnetosphere
Plasma density	Magnetosheath > Magnetosphere
Plasma temperature	Magnetosheath < Magnetosphere

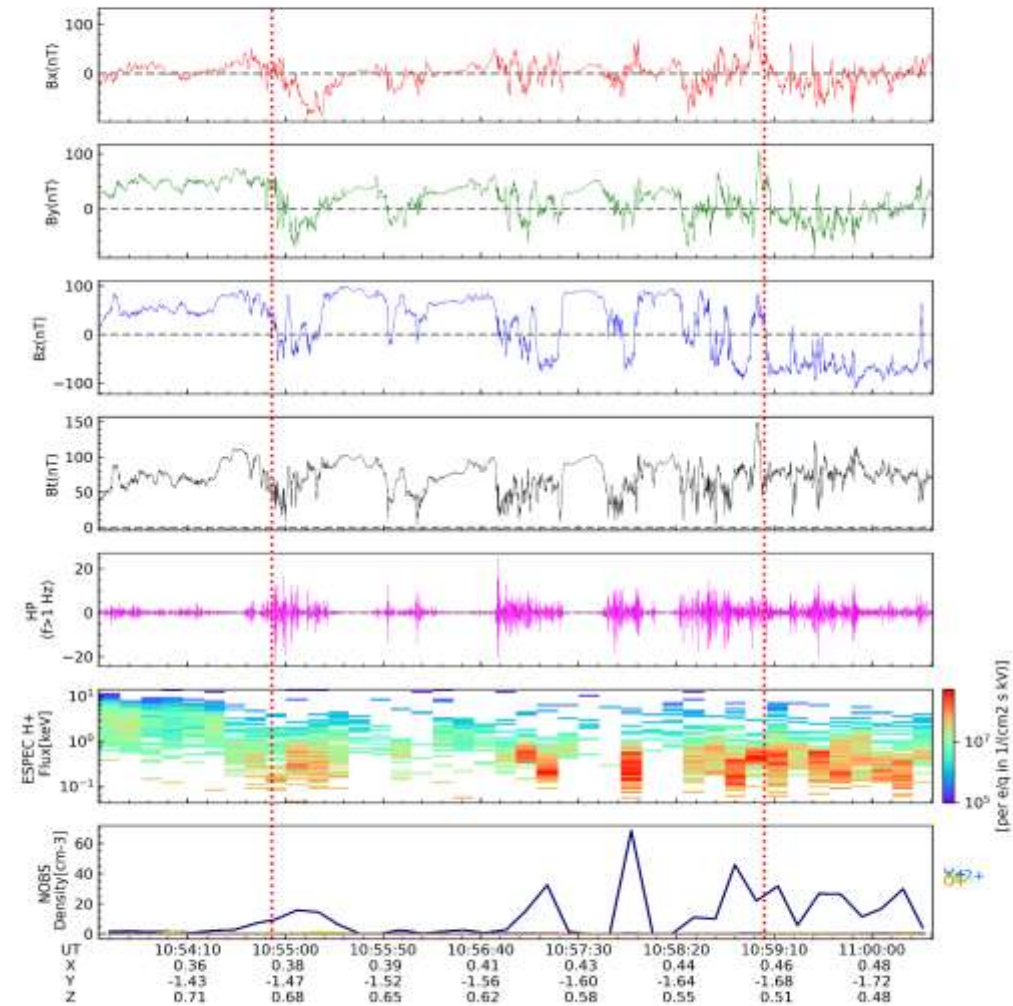
Linear magnetopause waves

time



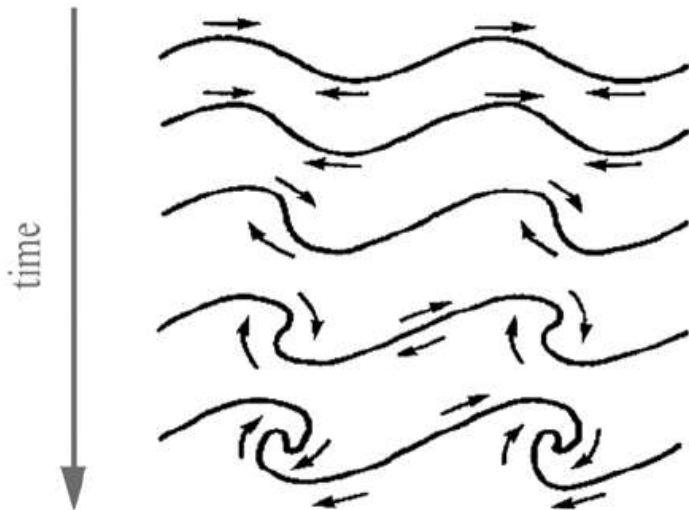
(b)

[Cushman-Roisin and Becker 2007]



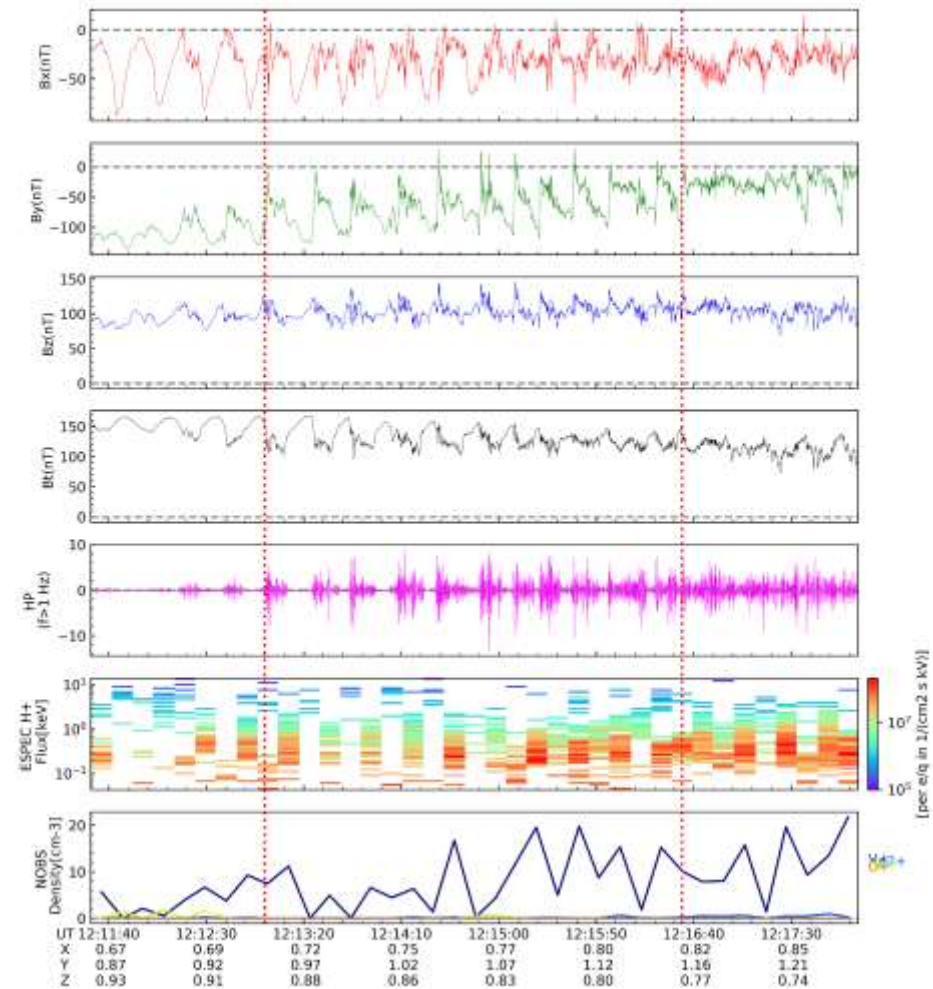
Box-like signature

Nonlinear magnetopause waves



(b)

[Cushman-Roisin and Becker 2007]



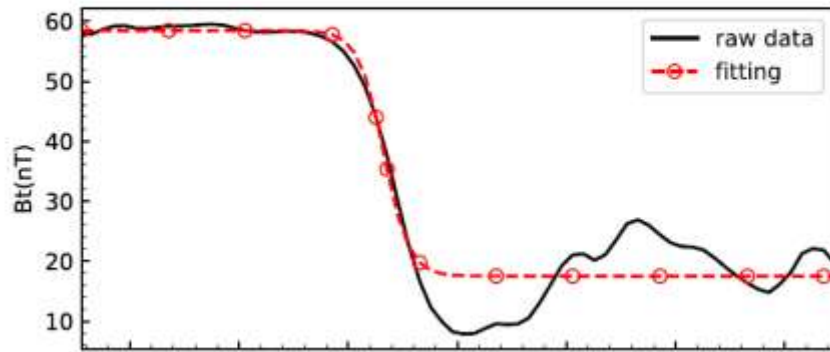
Sawtooth signature

3 Quantitative methods to identify linear vs. nonlinear K-H waves

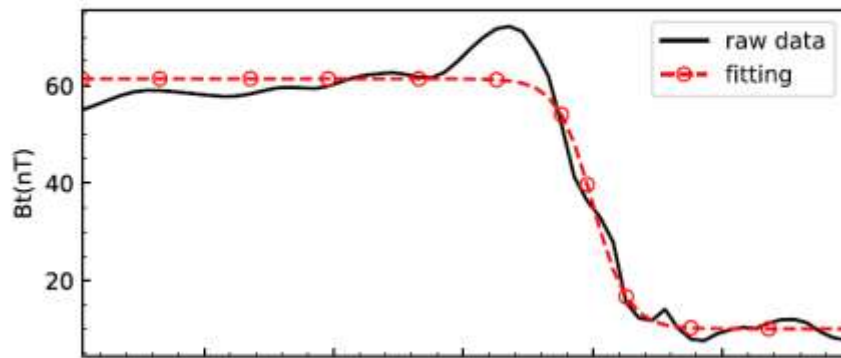


3.1 tanh fitting

Linear Case Fitting



Nonlinear Case Fitting



$$B(z) = B_0 \tanh\left(\frac{z}{L}\right)$$

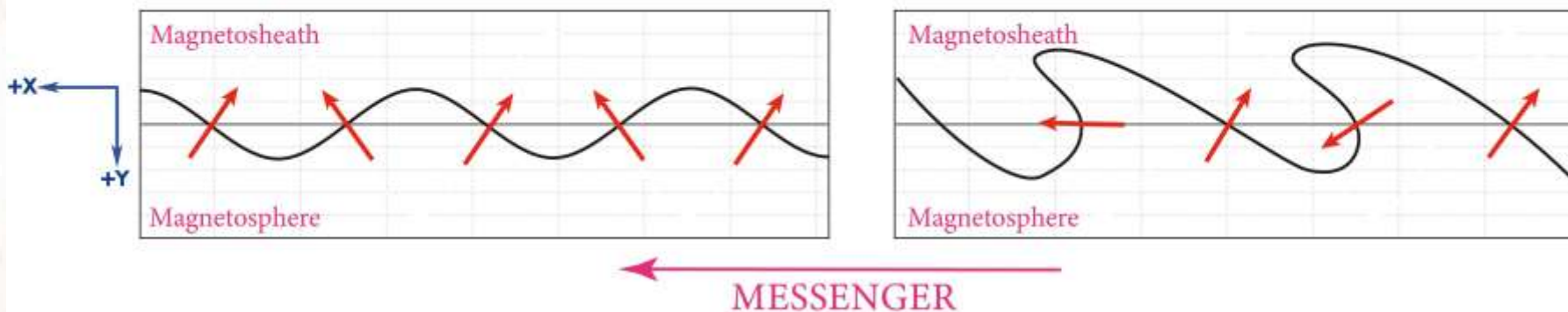
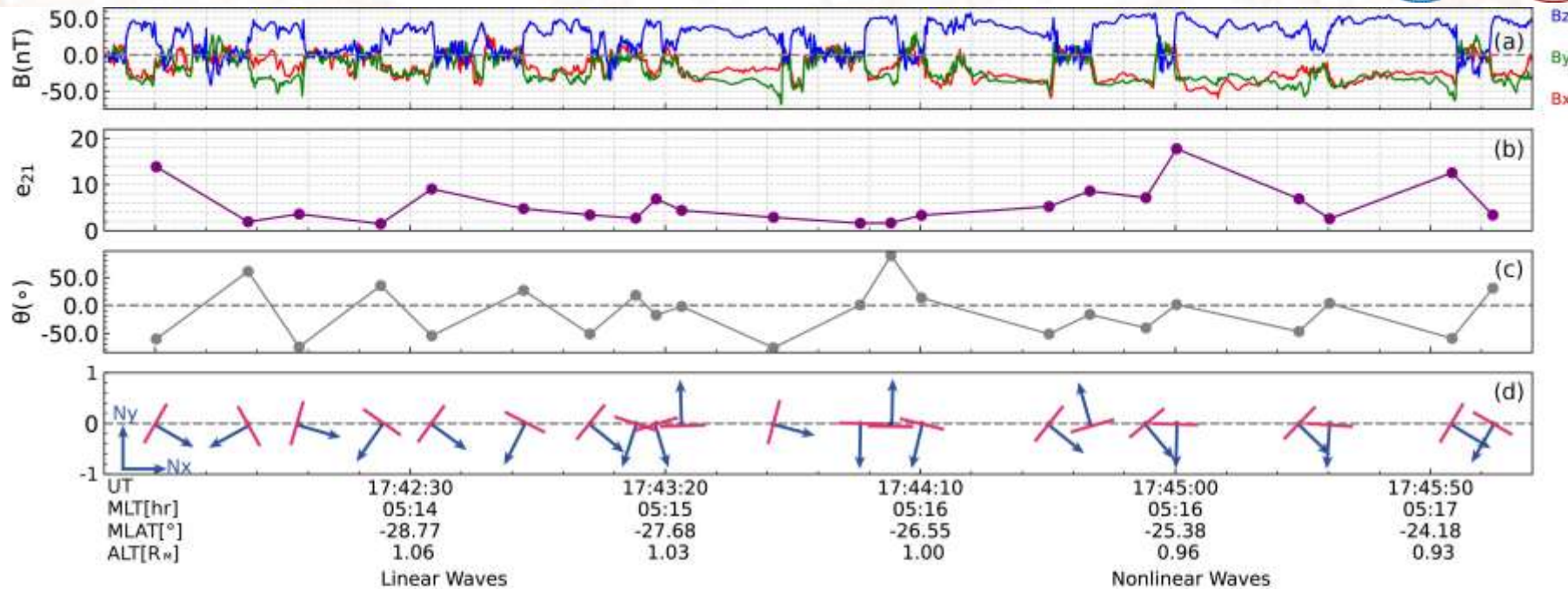
L: the half-thickness of the current sheet

B₀: the ambient magnetic field strength at the edge of the magnetopause current sheet

Bump: at least 15% above the modeled B₀

Bump: a deviation from the configuration of the magnetopause current sheet

3.2 Variations in the magnetopause normal direction

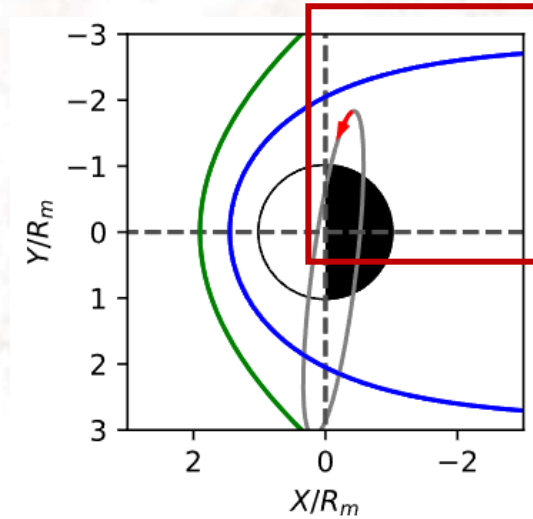
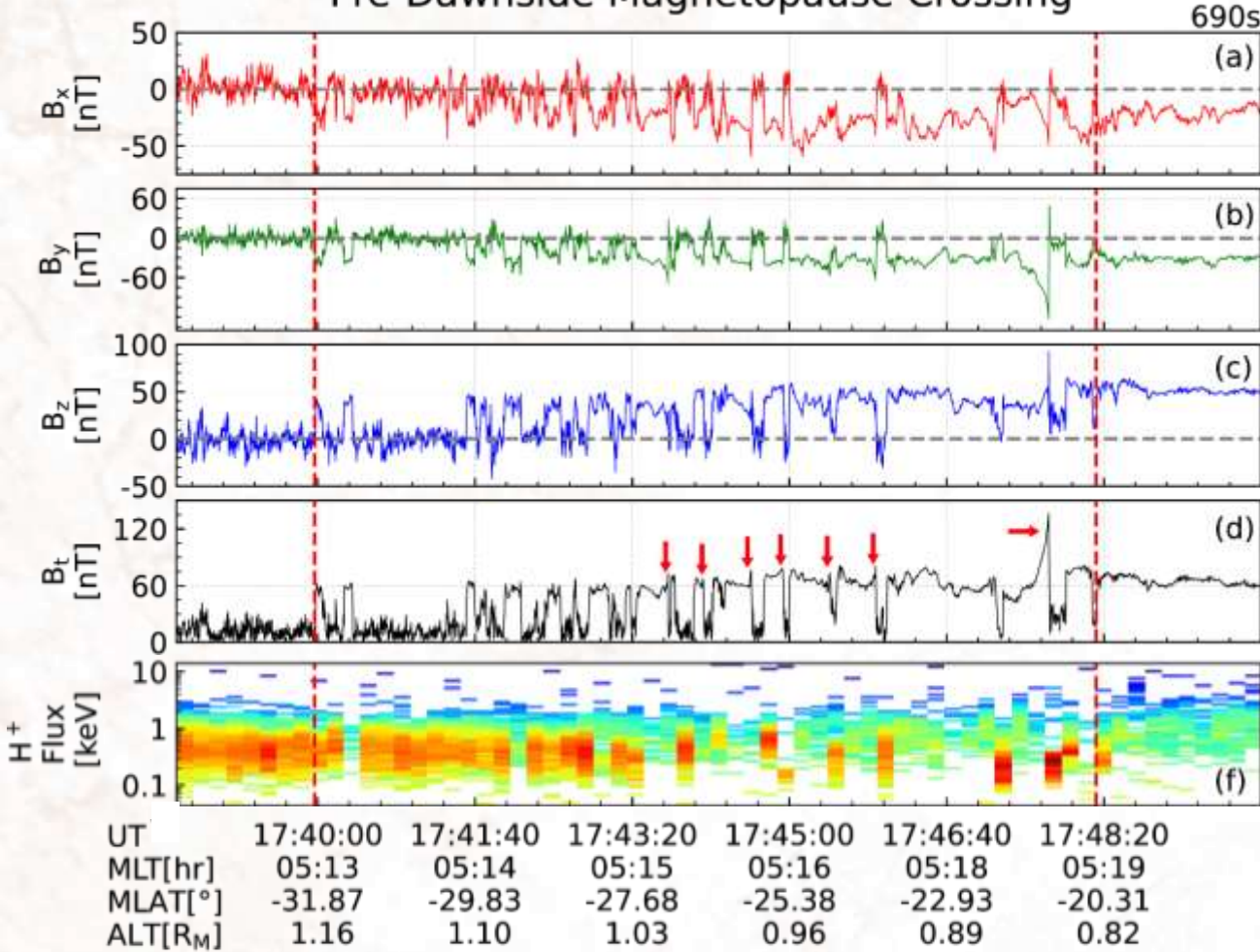


For linear-stage Kelvin-Helmholtz (K-H) waves, N_y maintains a consistent direction, while during the **nonlinear stage**, N_y exhibits sign reversals (positive/negative alternations).

4 Case Study • Pre-dawnside Magnetopause



Pre-Dawnside Magnetopause Crossing



K-H waves have not been observed in this area before.

Magnetic field	High-pass filter of Bt	Plasma Density
MSP>MSH	MSH>MSP	MSH>MSP

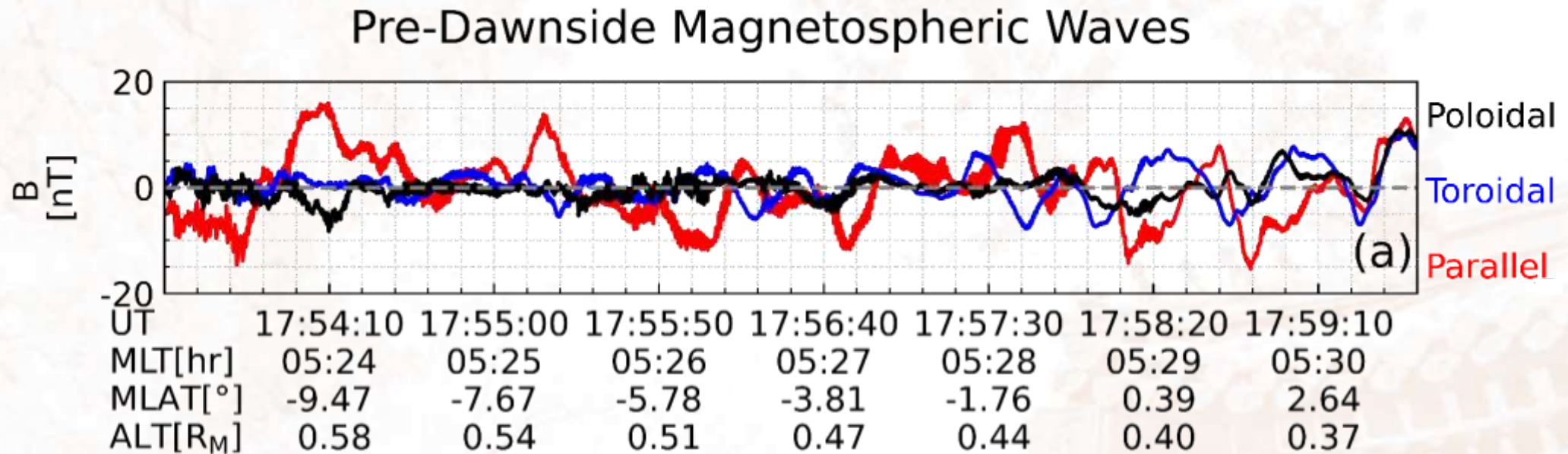
- Magnetic field intensity changes at least 40 nT
- Magnetopause crossing interval is at least 5s

Total: 17 KH waveforms
Period : ~40s

4 Case Study • Pre-dawnside Magnetosphere

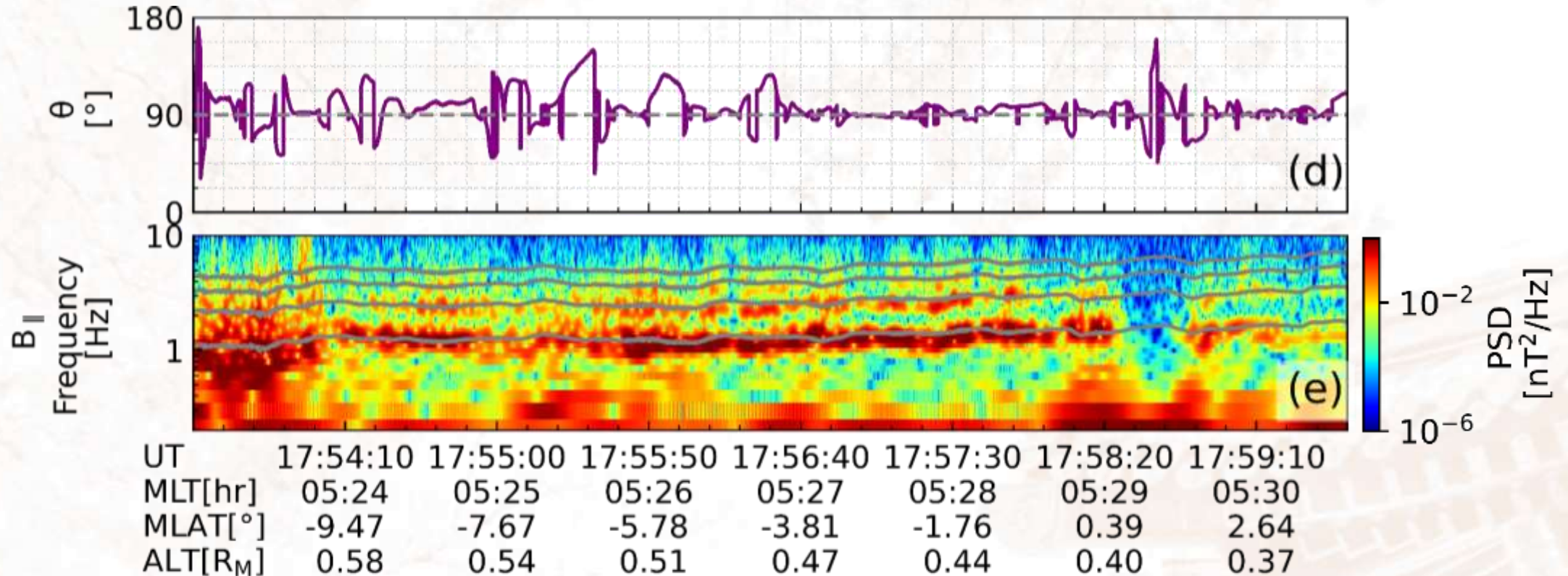


Energy Transport: 30mHz Compressional ULF waves



- 8 compressional waveforms
- **Period: ~35s** (similar to KH waves' period)

Particle Transport: Ion-Bernstein Modes

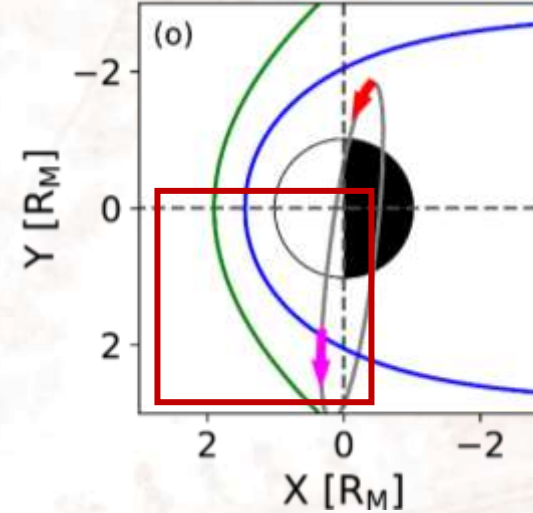
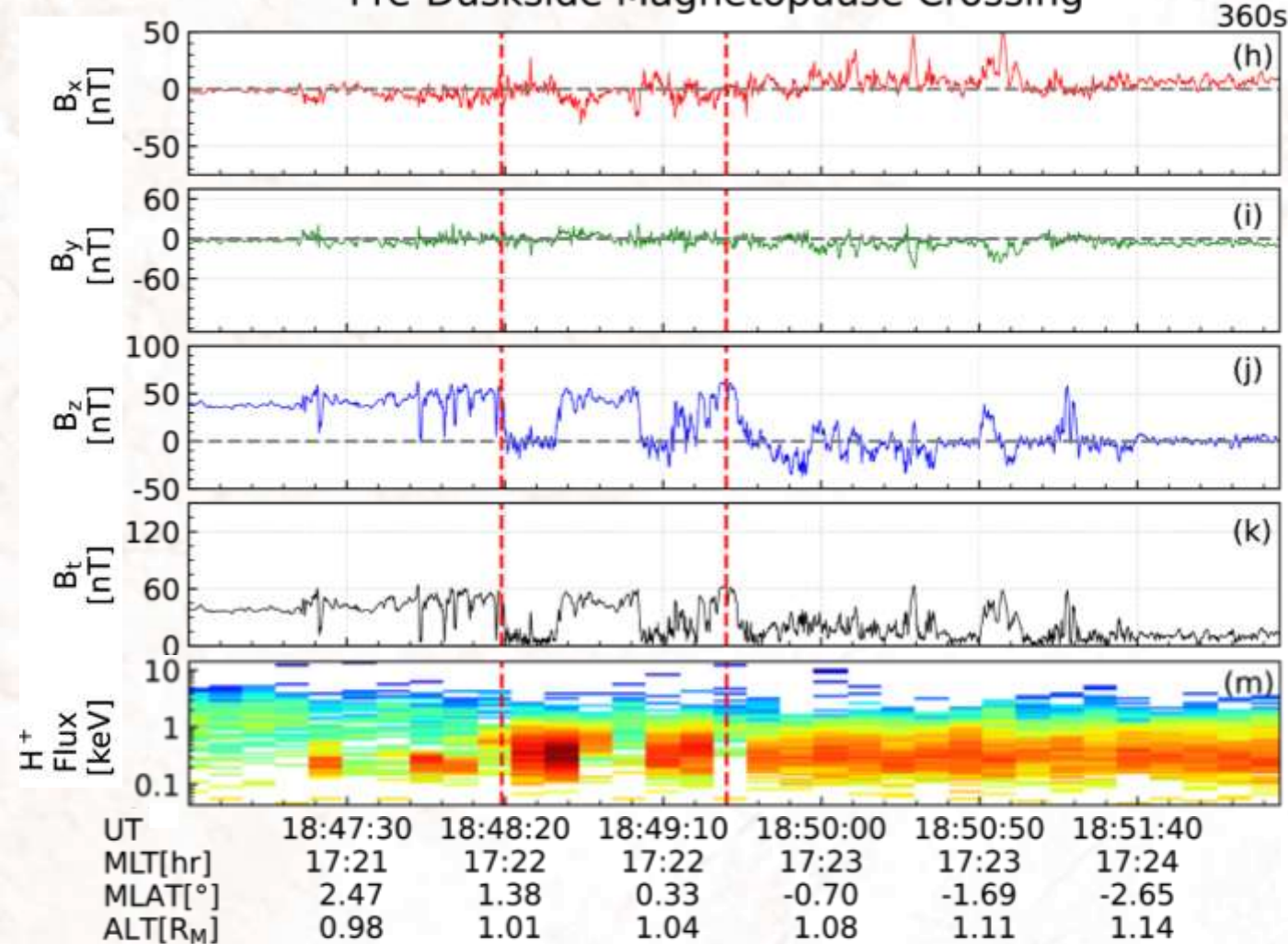


- ▶ Wave vectors are perpendicular to the background magnetic field
- ▶ Waves near **proton cyclotron and its harmonics**

4 Case Study • Pre-duskside Magnetosphere



Pre-Duskside Magnetopause Crossing



- 5 magnetopause crossings
- **No** compressional ULF waves
- **No** ion-Bernstein modes

5 Why K-H waves in our case are clearer on the pre-dawnside?

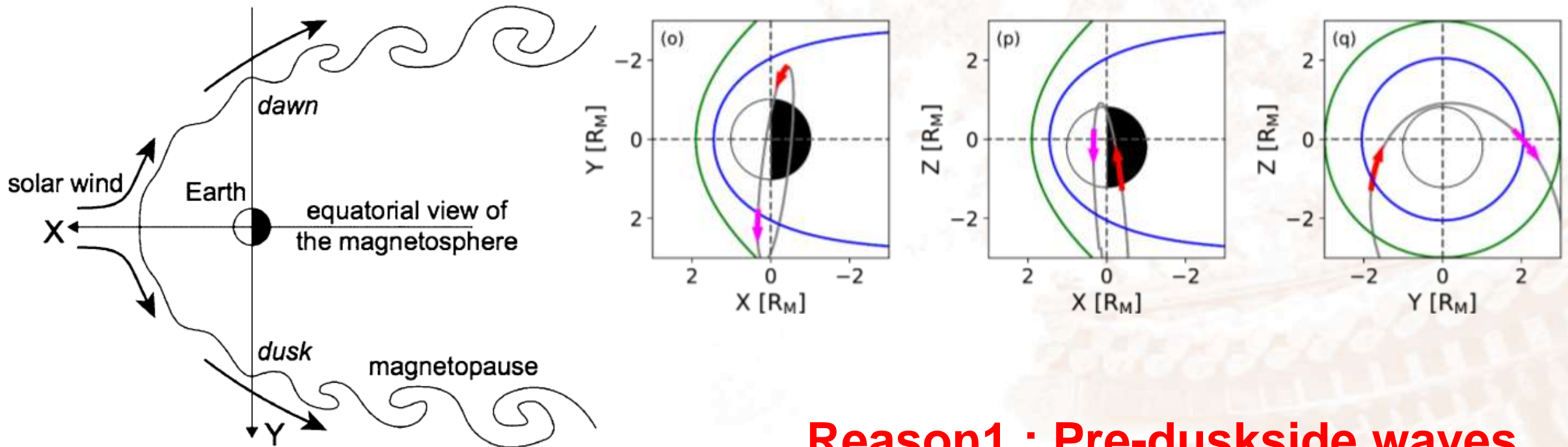


Fig. 10 Illustrating the expected evolution of the Kelvin-Helmholtz instability from a linear stage on the dayside magnetopause to a nonlinear stage on the flanks of the distant magnetotail

[D.G. Sibeck et al., 2011]

Reason1 : Pre-dusk side waves may not have fully developed

Reason2: a quasi-parallel shock on the dawnside and a quasi-perpendicular shock on the duskside



K-H waves are unstable when:

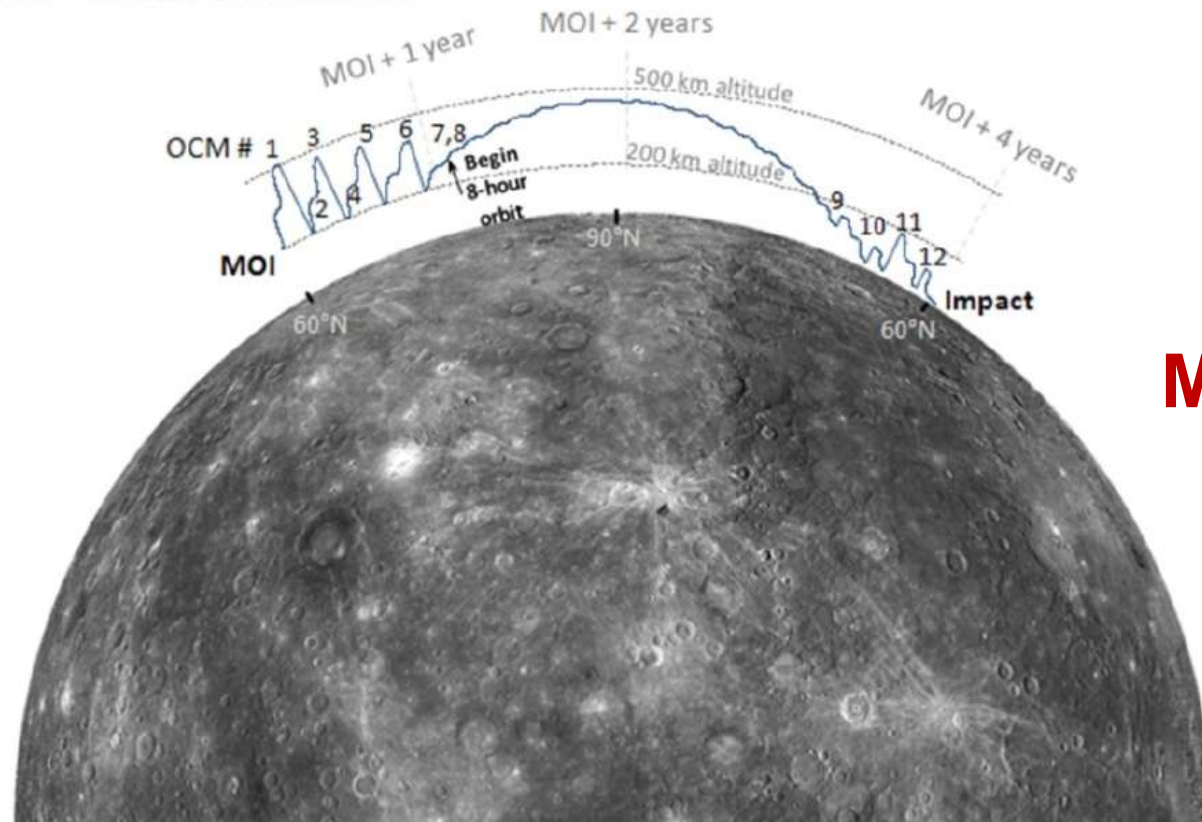
$$\frac{m_0 n_1 n_2}{n_1 + n_2} [\mathbf{k} \cdot \Delta \mathbf{V}]^2 > \frac{1}{\mu_0} [(\mathbf{k} \cdot \mathbf{B}_1)^2 + (\mathbf{k} \cdot \mathbf{B}_2)^2]$$

Upstream solar wind variability drives observed discrepancies.

	$\theta_{B_n} (^\circ)$	Bow shock	$B_k^* \text{ (nT)}$
Dawnside	23	Quasi-parallel	10.8
Duskside	55	Quasi-perpendicular	23.26

Consistent with Parker Spiral

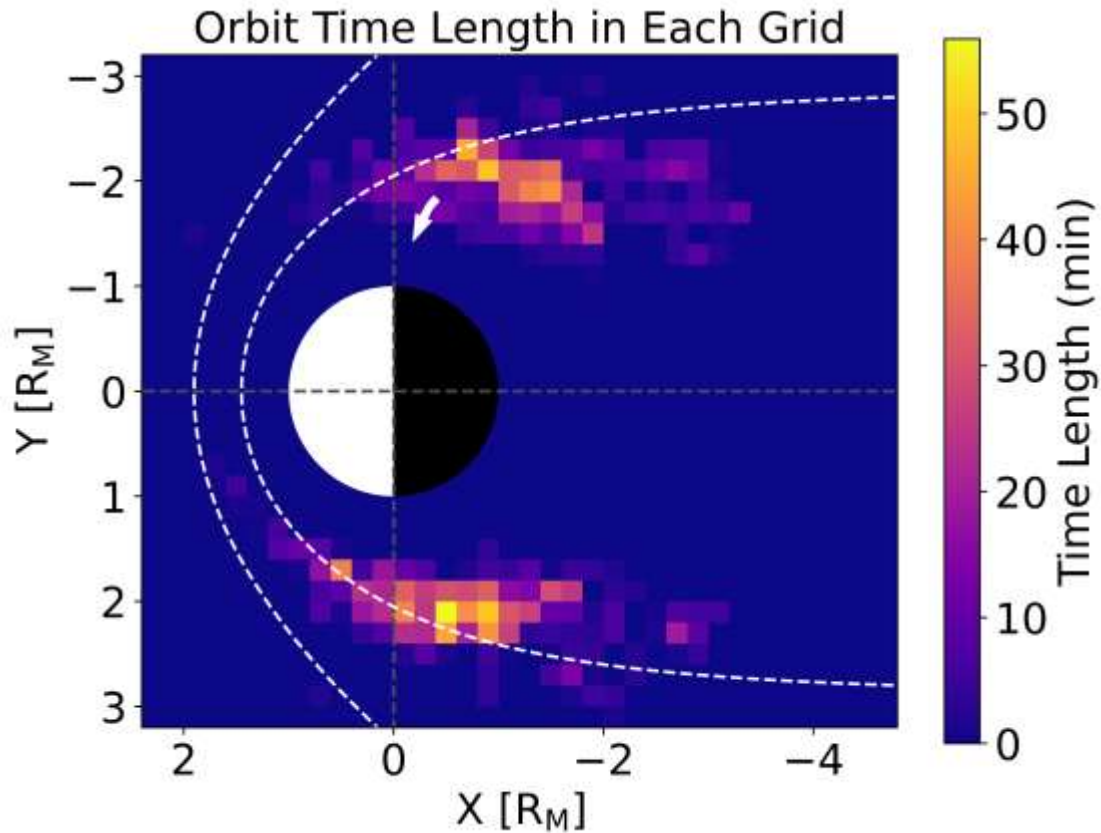
6 Why is Liljeblad's statistic lacking cases on the pre-dawnside?



MOI=Mercury Orbit Insertion
(2011.3.18)

Maybe because of the orbit

Figure 2. MESSANGER Periapsis Altitude during the Primary, XM1, and XM2 Orbital Phases. Periapsis Latitude Started at 60.0°N, Moved Northward to Peak at 84.1°N, and Then Moves Southward to 58.1°N at Mission End.



- MESSENGER orbit:
changed continuously after 2013.03.18

Liljeblad's statistic:

2011.3.24 - 2013.9.18

Our case:

2014.03.23

MESSENGER's orbits changed continuously after 18 March 2013. Liljeblad et al. (2014) primarily analyzed data collected before the orbital change.



6 Why K-H distribution in Liljeblad's statistical work is different from us?

- Orbit change
- Changes of IMF condition
- Maybe the criteria?